Ionic liquids for enhancing alkaline water electrolysis

Szilveszter Gábor Kéki

keki.szilveszter@gmail.com

Instituto Superior Técnico, Universidade de Lisboa, Portugal

October 2020

Abstract

Alkaline electrolysis is the most mature technology to produce hydrogen gas without using fossil fuels. Using electricity from renewable sources creates the opportunity to prepare hydrogen gas as a green energy carrier, helping the economy to switch from carbon-based to green and sustainable energy sources. However, nowadays 96% of hydrogen production is based on steam reforming, using fossil fuels. To make electrolysis competitive towards steam reforming, enhancing the efficiency of hydrogen and oxygen evolution reactions (HER and OER) is essential. Besides, by selecting suitable electrocatalytic materials, the activation overpotential could be decreased by electrolyte additives, such as room temperature ionic liquids (RTILs). Improved HER kinetics in the presence of RTILs has been previously confirmed in both acidic and alkaline solutions. As RTILs could be easily modified, the effect on HER and OER kinetics of new types of RTILs, namely: a) 3-Ethyl-1-methylimidazolium chloride (C2); b) 3-Butyl-1-methylimidazolium chloride (C4); c) 3-(2-Methoxyethyl)-1-methylimidazolium chloride (C1OC2); and d) 3-(2-Ethoxyethyl)-1-methylimidazolium chloride (C2OC2), was examined in this study. Cyclic voltammetry, linear scan voltammetry, and chronoamperometry are carried out at different temperatures between 25 ºC and 80 ºC. using Pt electrodes to study the effect of the addition of a small amount (1 vol.%) of the listed RTILs on HER and OER kinetics in alkaline solution. Kinetic parameters are calculated. Furthermore, gas volume measurements were done to compare the gas production in pure 8 M KOH solution, and the gas production with the addition of the chosen RTIL in a small-scale alkaline electrolyser.

1. Introduction

One of the greatest challenges of humanity in the 21st century, is to minimise the impact of global warming. The Paris Agreement's long-term temperature goal is to “keep the increase in global average temperature to well below 2ºC above pre-industrial levels; and to pursue efforts to limit the increase to 1.5 ºC, recognizing that this would significantly reduce the risks and impacts of climate change [3].

The International Energy Agency (IEA) provides a sustainable development scenario (SDS) to estimate energy consumption in 2040. The SDS is fully in-line with the long term objectives of the Paris Agreement and is aiming to maintain the global energy consumption on the current level (2017, 13972 Mtoe), meanwhile cutting drastically CO_2 emission (32.5 → 17.5 Gt energy-related CO_2 emission) by increasing the share of renewable energy (RE) sources in the final energy consumption [7].

Currently, 50% of the final energy consumption is related to heat and ~28% related to the transport sector, which can be interpreted to global CO_2 emissions share. Thus, heat production is responsible for 33% and the transport sector for 22% of the global CO_2 emission. According to the SDS, we have to rise RE share in the heating sector up to 25% from 10%; and in the transport sector up to 19% from 3.5%, meanwhile the RE shares in electricity production should rise to 66% (from 25%) until 2040 [7]. However, according to IEA’s data, in 2017 the shares of Solar photovoltaic (PV) and Wind energy in electricity generation were only 1.7% and 4.2%, respectively [7]. Furthermore, these RE sources are already making grid-stability problems due to their high temporally fluctuations [9, 10]

Power to gas (P2G) technology enables the storage of electric energy in the form of hydrogen or methane. Both H_2 and methane can be used as fuel for transportation (in internal combustion engines and fuel cells) and heating purposes. So far, the pipeline system for natural gas is already installed worldwide; hence in the close future, P2G could offer a large-scale long-term storage option for electricity, which can solve grid stability issues related to Solar PV and Wind energy.

Water electrolysis is used in P2G plants for using electricity to transform water into hydrogen (and oxygen). Today primarily alkaline and polymer membrane (PEM) electrolysis is used in applications. Alkaline electrolysis is the most used technology, due to its lower cost, and better endurance. But, currently, 96% of hydrogen is produced by steam reforming, using fossil fuels. To compete with fossil-based hydrogen production technologies, the efficiency of electrolysis needs to be improved.

The activation overpotential can be decreased by selecting properly the electrode material, or by, what is the topic of this work, modifying the electrolyte by additives. In this work, four different methylimidazolium-based ILs were tested as

electrolyte additives [1]. The positive effect of methylimidazolium-based and other ILs as electrolyte additives on HER kinetics have been reported previously [2, 3, 4]. However, this effect of ILs is poorly described. The experiences with ILs and the potential explanations of their catalytic behaviour on HER and OER are the following:

- Investigation towards the alkyl chain length in Imidazolium$^+$ suggests that 4 carbon-atom long alkyl chain is the optimum length. A shorter chain would protect less the electrode surface, a longer chain would block too much of the electrochemically active surface area (ECAS) [5].
- Decreasing resistance related to mass and charge transfer also decreases the overall impedance and enhances HER kinetics [2, 3].
- Provides better adsorption on the electrode surface by helping cations to lose their solvation layer with the non-polar alkyl chains [6].
- Imidazolium$^+$ acts as a proton donor/acceptor, thus providing a better proton donating effect and participating in the charge transfer reaction [7].
- Cations of the IL form organised channels, perpendicular to the electrode surface [4].
- Inhibits Pt dissolution and suppresses the formation of nonactive oxygenated species on the electrode surface [5].
- Imidazolium$^+$ is competing with the adsorbed H_2 molecules, thus facilitating H_2 desorption. Since imidazolium$^+$ acts as an H^+ donor and acceptor, it is participating in the charge transfer process and does not block active sites. These and other results indicate that the IL changes the electrolytic double layer (EDL) structure [6].
- The catalytic effect is related to the imidazolium$^+$ cation, which can be located near the anode in case of low potential, because at low potentials a charge-separated layer structure forms around the anode, whereas the proposition of the ions depends on the magnitude of the electrode surface [5].
- The shorter the alkyl chain, the slower the decomposition of the IL [8].

In this study, four different ILs were tested as additives during HER and OER.

2. Experimental

The goal of this study is to observe the effect of adding different ionic liquids (ILs) to the electrolyte on hydrogen evolution reaction (HER) and as well on oxygen evolution reaction (OER) during alkaline water electrolysis. All of these four IL have chloride (Cl^-) anion, while the cations are different methyl-imidazolium-based cations. Namely, the four ILs are: a) 3-Ethyl-1-methylimidazolium chloride (C2); b) 3-Butyl-1-methylimidazolium chloride (C4); c) 3-(2-Methoxyethyl)-1-methylimidazolium chloride (C1OC2); and d) 3-(2-Ethoxyethyl)-1-methylimidazolium chloride (C2OC2).

2.1. Electrochemical measurements

8 M KOH (AppliChem Panreac 85%) solutions were prepared with Millipore water. After that, 1 vol % of one of the four studied ILs was added to the solutions. However, since C2mim-Cl and C4mim-Cl were in the solid phase at room temperature (their melting point is ca. 70 ºC), mass equivalent to 1 vol.% of IL (determined using the density of ILs at their melting point) was added to the solution. 50 mL of electrolyte was used for the electrochemical measurements.

The potentiostat (EG&G Princeton Applied Research Potentiostat/Galvanostat 273A) was operated by Power Suite software. In the electrochemical cell the working electrode was a Pt foil (Metrohm 6.0305.100), surface area: 1 cm^2), the reference electrode was a calomel electrode with 3.5 M KCl (HANNA instruments HI5412, 3.5 M KCl), and the counter electrode was a Pt mesh of 50 cm^2 surface area. All potentials are converted to the reversible hydrogen electrode (RHE) scale. Both HER and OER measurements were performed without adding IL and then with the addition of IL.

In the case of HER, cyclic voltammetry (CV) was performed 2 times with 3 consecutive cycles from -0.176 V to 1.517 V at 25 mV s^{-1}. Chronoamperometry (CA) was performed at -0.183 V for 3 min. Linear scan voltammetry (LSV) was performed from OCP to -0.383 V at 2 mV s^{-1} at 25 ºC, 40 ºC, 50 ºC, 60 ºC, 70 ºC and 80 ºC. Finally, stability tests were performed by chronoamperometry at a potential of -0.283 V for 7200 s, at 25 ºC and 80 ºC. The electrolyte solutions were saved for FTIR analysis.

In the case of OER, cyclic voltammetry was performed 2 times with 3 consecutive cycles from -0.117 V to 2.117 V at 25 mV s^{-1}. Linear scan voltammetry was performed from OCP to 2.117 V at 2 mV s^{-1} at 25 ºC, 40 ºC, 50 ºC, 60 ºC, 70 ºC and 80 ºC. The stability test was performed by chronoamperometry at a potential of 1.917 V for 7200 s at 25 ºC and 80 ºC. The solutions were saved for FTIR analysis.

2.2. Volume measurements

With the IL whose addition lead to the best HER and OER performance, the generated gas volume measurement was done by a Ritter Miligascounter type MGC-1 PMMA. The electrodes were Ni electrodes with a surface area of 22.4 cm^2 for each electrode. 150 mL of 8 M KOH solution with 1 vol.% of IL added were filled in an air-sealed plastic beaker. The gas production was measured first during a two-hour galvanostatic electrolysis when a constant current was applied, and secondly during a two-hour-long potentiostatic electrolysis when a constant potential was applied. The current and the potential were controlled by EG&G Princeton Applied Research Potentiostat.

3. Results and discussion

3.1. Degradation of the studied ILs

During the LSV test at different temperatures – from 25 ºC to 80 ºC – the degradation of ILs was detected. Over 40 ºC the solution started to turn to foggy white or yellow, then it turned to an opalescent orange and red colour. Finally, the solution held a red colour, then cleared out, and dark red oil like droplets were formed at the top of the solution.

3.2. HER studies

3.2.1. HER Cyclic Voltammetry

The pure 8M KOH solution shows a small oxidation reaction before the HER starts to occur (**Figure 1**). This small oxidation bump was previously observed in other studies and is related to Pt oxidation. The addition of the ILs significantly increased the cathodic currents recorded at -0.2 V (-3.8 mA for pure KOH; -10.2 mA for C2; -9.7 mA for C4; -11.7 mA for C1OC2; -9.8 mA for C2OC2) and the onset potential for the HER (assuming -1mA as the reference current value of the start of the reaction) was shifted to lower overpotentials (-0.119 V for pure KOH; -0.03V for C2; 0.014V for C4; -0.029 V for C1OC2; -0.036 V for C2OC2). ILs with similar functional groups (alkyl groups C2, C4, and ethoxy groups C1OC2, C2OC2) showed similar curves.

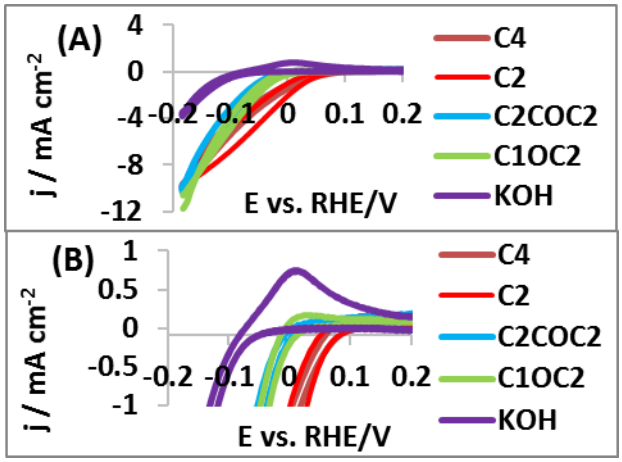

Figure 1. Cyclic voltammetry (CV) curves recorded in 2 sets with 3 consecutive cycles from -0.176 V to 1.517 V at 25 mV s^{-1}. The second set is shown for (A) Comparison of the pure 8 M KOH solution and the addition of four different types of ILs; (B) Comparison of the onset potential of the solutions containing each of the four ILs with the pure 8 M KOH solution.

3.2.2. HER Linear Scan Voltammetry

If the current density would only be a function of the potential and temperature (for a given composition of the solution), the curves would look similar to the result of KOH (**Figure 2A**). However, above 40 ºC, RTILs start to decompose, and this has a negative effect on the current densities (**Figure 2C**). Only C2 RTIL showed rising current densities with the elevation of temperature (**Figure 2B**). This can be explained, by the observations of Gao et al., where they found that the shorter the chain-length on the imidazolium^{+} ring the more stable the IL is [8]. Therefore, probably the C2 IL decomposes slower hence the negative effects are lower than the positive effects from the temperature rising, and the polarisation curves of C2 added solution are parallel with pure KOH results.

On the other hand, at 25 ºC, each RTILs significantly increased the current densities, as well as decreased the onset potential. And even though the decomposition has a significant negative effect at 80 ºC, each IL also significantly performed better than the pure KOH solution (except for except C4 IL) (**Figure 3**).

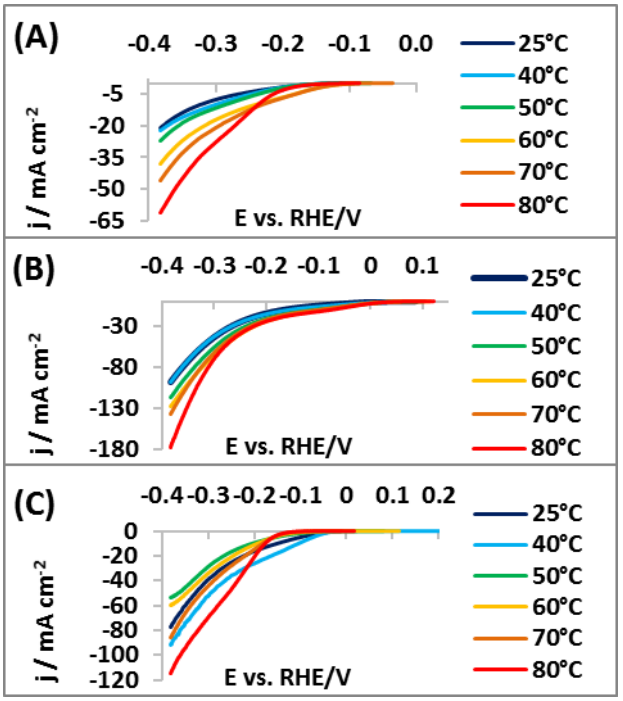

Figure 2. Linear scan voltammetry performed from OCP to -0.383 V at 2 mVs^{-1} at 25 ºC, 40 ºC, 50 ºC, 60 ºC, 70 ºC, and 80 ºC in (A) IL-free 8M KOH electrolyte and with the addition of (B) C2 IL and (C) C1OC2 IL.

The addition of C2 and C1OC2 ILs to KOH solution at 25 ºC resulted in better performance comparing to the results of KOH solutions without adding ILs at 80 ºC (**Figure 4**). Which means with these IL the heating up time could be avoided, which would decrease the starting up time of alkaline electrolysers.

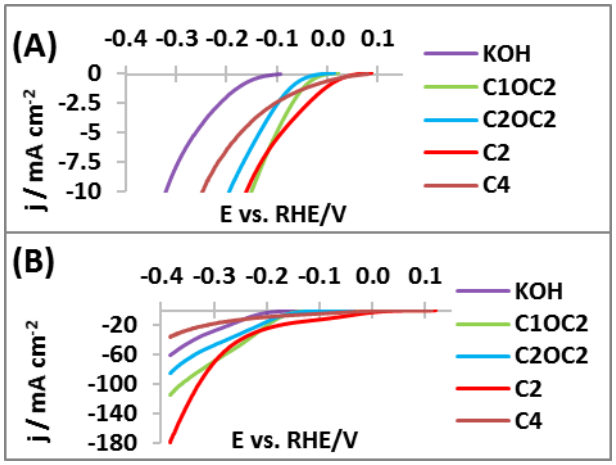

Figure 3. A) Comparison of the onset potential in 8 M KOH with ILs and in pure 8 M KOH solution at 80 ºC. (B) Comparison of the polarisation curves in 8 M KOH solution before and after addition of each of the four ILs at 80 ºC.

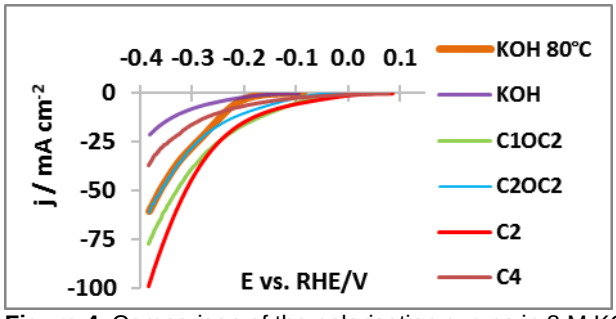

Figure 4. Comparison of the polarisation curves in 8 M KOH solution before and after addition of four different types of ILs at 25 ºC with the polarisation curve in 8 M KOH at 80 ºC**.**

3.2.3. Tafel plots

The data related to HER in pure 8M KOH is shown in **Table 1**. The slope is over 0.120 V/dec, which indicates that the rate-determining step (RDS) is the first electron transfer reaction, which is the Volmer reaction. At 25 ºC, the pure 8M KOH solution had the lowest slope. On the other hand, the j_0 was significantly improved, ca-5 to 10 times, upon the addition of the ILs. The highest j_0 values are connected to C1OC2 IL. The E_{10} was also reduced by 50% or more by the C2 and by the C1OC2 ILs. The j_{150} current density also increased significantly, the best result achieved with the addition of C2 and by the C1OC2 ILs.

Table 1. Comparison of the kinetic parameters of HER after the addition of 4 different IL at 25 ºC.

25 ºC	Tafel slope / V dec^{-1}	j_0 / mA cm^{-2}	E_{10} / mV	j_{150} / mA cm^{-2}
KOH	0.191	0.24	321	0.52
C1OC2	0.256	2.85	150	9.92
C2OC2	0.229	1.37	195	6.15
C2	0.21	1.66	161	8.95
C4	0.251	1.04	248.2	4

At 80 ºC, C2 presented the lowest slope. The j_0 was increased in general, the C1OC2 and the C2 ILS have outstanding results. The highest j_{150} current density was also achieved with the addition of C2 IL, results shown in **Table 2**. C4 leads to the lowest currents at 80 ºC, with poorer performance than the plain KOH solution. This might be related to the degradation of C4 ionic liquid with the temperature. The comparison of Tafel plots at 25 ºC and at 80 ºC is shown in **Figure 5**.

Table 2. Comparison of the kinetic parameters of HER after the addition of 4 different IL at 80 ºC.

80 ºC	Tafel slope / V dec^{-1}	j_0 / mA cm^{-2}	E_{10} / mV	j_{150} / mA cm^{-2}
KOH	0.241	1.45	236	0.58
C1OC2	0.379	8.82	176	3.28
C2OC2	0.323	5.56	182.8	3.83
C2	0.218	2.88	70.7	16.9
C4	0.35	2.2	220.5	6.45

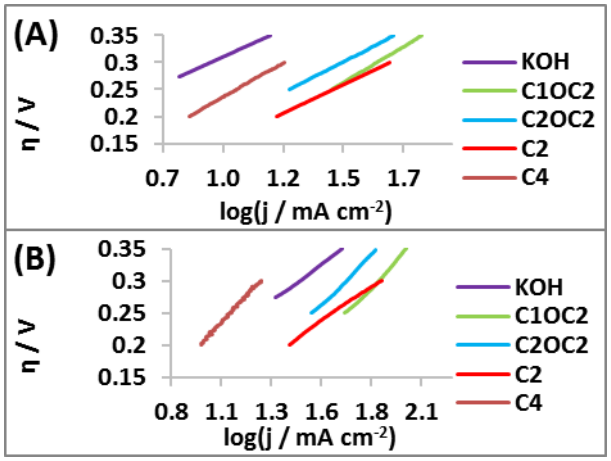

Figure 5. Comparison of the Tafel plots of HER (A) at 25 ºC and (B) at 80 ºC.

Further characterisation of the HER was performed by considering the variation of j_0 with the temperature, allowing the calculation of activation energies, E_a. A simple Arrhenius relation, Eq. 1, where A_i is the Arrhenius pre-exponential factor, E_a the activation energy, R is the universal gas constant 8.314 $\frac{J}{K \cdot mol}$ and T is the temperature in Kelvin - was applied, with the resulting plots being presented in **Figure 6A**.

$$\ln(j_0) = A_i - \frac{E_a}{R \cdot T} \quad (1)$$

The obtained HER E_a values are shown in **Figure 6B**. The addition of C1OC2 increased significantly the HER E_a, C2OC2 IL slightly increased HER E_a, meanwhile, the C4 IL slightly decreased it, and the C2 IL significantly reduced the HER E_a.

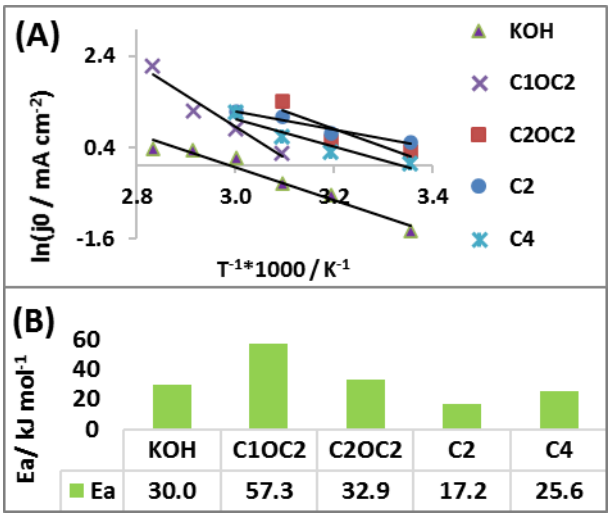

Figure 6. (A) HER Arrhenius plots for 8 M KOH solution without and with the addition of C1OC2, C2OC2, C2, and C4 ILs and (B) the corresponding HER activation energies.

3.2.4. HER stability test

At 25 ºC at the beginning of the stability test, the C2 IL started at the highest current density, comparing to KOH 20 times higher. However, the high current density was jumping down rapidly, after about 3500 s the currents density of C2 got lower than the current density of KOH. The C2OC2 IL has a similar descending trend as C2, at the end of the test both of them have smaller current densities than KOH. The

highest final current was obtained by C1OC2 IL, barely over 4 mA cm^{-2}. The C4 IL reached a similar final current density as KOH, but it started, much higher, and the current density reduction was slower comparing to KOH (**Figure 7A**).

At 80 ºC the highest starting current density was achieved by the C1OC2 and the C2OC2 ILs. These IL represent fast jump down as well as C2 behaved at 25 ºC. These two IL also had lower current densities than KOH by the end of the test. The C2 had a higher starting current density than C4 and KOH and show a descending trend until about 4700 s, after that the current density starts to slowly increase step by step, and show an increasing trend at the end of the test. This strange increasing trend is also observed from 300 s with the addition of C4. Namely, C4 made a more rapid elevation followed by a more rapid decrease. The most consistent current density was achieved by C4, which dominates the stability test result after around 1000 s and has a generally increasing part until 5100 s after that it shows a descending trend until the end of the test (**Figure 7B**).

This strange behaviour of the stability test curves can be explained by a measurement failure. However, the strange behaviour was found twice with the addition of C2 and C4 IL. Another explanation can be, that different intermediates of the degradation of these IL liquids have a different effect on the HER. The intermediates at the beginning have a negative influence on HER, and the later intermediates have a positive effect on HER. Also, the reactions of IL degradation can influence the measured current density.

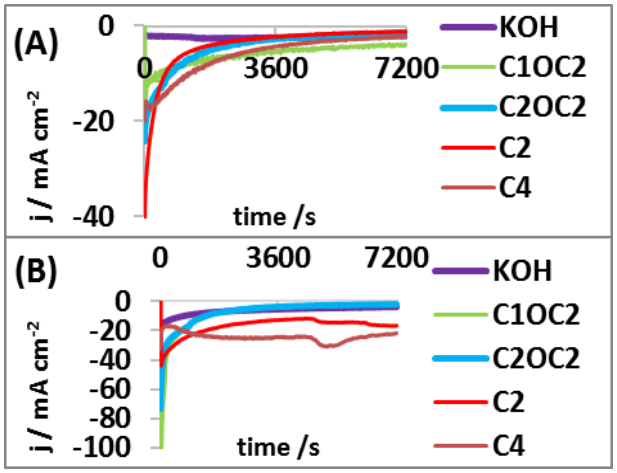

Figure 7. 2h-long HER stability test in 8 M KOH solution before and after the addition of C1OC2, C2OC2, C2, and C4 ILs on -0.283 V: (A) at 25 ºC ; (B) at 80 ºC.

3.3. OER studies

3.3.1. OER Cyclic Voltammetry

CV results were run in duplicate and for 3 consecutive cycles, with the second cycles being show in **Figure 8**. A significantly higher current density peak was observed in the pure KOH solution than in C4, C1OC2, and C2OC2 ILs. The C1OC2 and the C2OC2 curves have very similar trends and peaks as in the CV presented in Fig. 1. The other two ILs, C2 and C4 have very different trends and peaks. C2 also has a significantly higher peak than KOH. This dissimilar trends and peaks for ILs with analogue function groups (namely -ethyl and -butyl groups) in **Figure 1** and **Figure 4** was somewhat surprising.

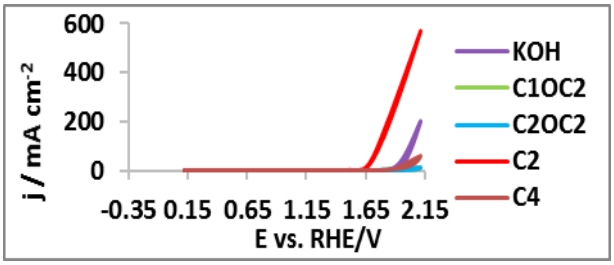

Figure 8. Cyclic voltammetry curves (second cycle) recorded from 0.125 V to 2.12 V at 25 mV s^{-1} in the 8 M KOH solution before and after addition of C1OC2, C2OC2, C2, and C4 ILs.

3.3.2. OER Linear Scan Voltammetry

The effect of ILs on OER was not studied before. ILs were starting to decompose with the elevation of temperature, as well as during HER measurements. The results of C2 IL are way too much better in terms of current density orders of magnitude higher comparing to values with pure KOH and other ILs, thus, during those measurements, some failures probably happened and C4 data was taken out from the comparison chart. Other ILs significantly worsen OER kinetics, which resulted in smaller current densities.

On the other hand, LSV records at 25ºC - below 1.9 V - the OER reaction starts earlier with the addition of ILs shown in **Figure 9**. This can be explained by the assumption that IL ions would form a charge-separated layer formation, with a changing anion-cation rich layer at the electrode surface, whereas the proposition of the ions depends on the magnitude of the electrode surface. Therefore, on lower potential the concentration of the active cations close to the positively charged anode is higher, hence their catalytic effect is higher as well.

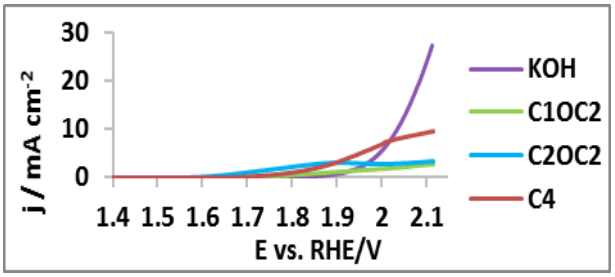

Figure 9. Comparison of the polarisation curves of OER at 25 ºC in 8 M KOH solution before and after the addition of C1OC2; C2OC2, and C4 ILs.

During LSV measurements C1OC2 IL appeared the most stable. The curves are in accordance with the temperature increase. The current densities during LSV at 25 ºC followed the order C1OC2 < C2OC2 < C4, but the pure KOH outperformed each of them. C2 current density dropped drastically at 80 ºC. At 80 ºC, each IL performed worse than the pure KOH solution see at **Figure 10**.

On the other hand, the OCP shifted to a more negative value - see at **Table 3** - and the current density started to slowly increase much earlier – at 0.5V - comparing to pure KOH solution where the onset point is 1.5 V.

Table 3. Comparison of the OCP of the different solutions at 25 ºC and 80 ºC

	OCP vs. RHE / V	
	25 ºC	80 ºC
KOH	1.518	1.305
C1OC2	0.984	0.479
C2OC2	0.973	0.538
C2	1.282	0.483
C4	1.125	0.510

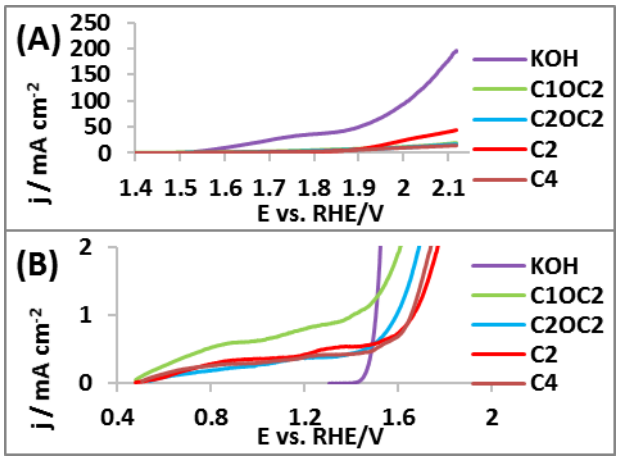

Figure 10. (A) Comparison of polarisation curves of OER at 80 ºC in pure 8nM KOH solution, and upon the addition of four different ILs; (B) Comparison of the OER onset potentials.

3.3.3. OER Tafel plots

At 25 ºC, the addition of each ILs increased the slope. The highest increment was done by C2OC2 almost 10 times higher, the lowest increment was done by C4 which almost doubled the slope. Every ILs increased j_0, similarly as in HER, but during OER the increment is more significant. Each ILs decreased the E01, the reduction was minor in connection with C4 and C1OC2 ILs, meanwhile the C2OC2 reduced E01 by 33%, and the C2 reduced it by 45%. Each IL significantly rose the j_{500} current density see in **Table 4**. At 80 ºC, the slope was reduced only by C2. Each IL reduced the j_0, C2 the most. The E01 was reduced only by C1OC2 and none of the ILs increased j_{500}, whereas C2 performed the worst (**Table 5**).

Table 4. Comparison of kinetic parameters of OER after the addition of 4 different IL at 80 ºC.

at 80 ºC	Tafel slope / V dec^{-1}	j_0 / mA cm^{-2}	E_{01} / mV	j_{500} / mA cm^{-2}
KOH	0.457	1.819	263	30.6
C1OC2	0.693	0.877	169	3.99
C2OC2	0.560	0.455	353	2.92
C2mim	0.180	0.002	425	1.62
C4mim	0.370	0.097	500	1.99

The comparison of Tafel plots at 25 ºC and at 80 ºC are shown in **Figure 11**.

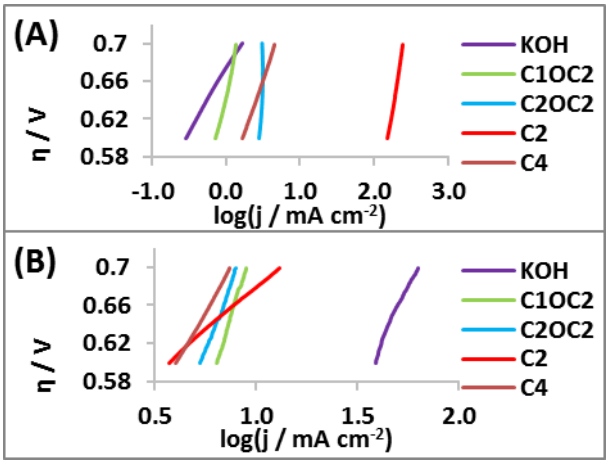

Figure 11. Comparison of the Tafel plots of OER (A) at 25 ºC and (B) at 80 ºC.

Table 5. Kinetic parameters of OER after the addition of 4 different IL at 25 ºC

at 80 ºC	Tafel slope / V dec^{-1}	j_0 / mA cm^{-2}	E_{01} / mV	j_{500} / mA cm^{-2}
KOH	0.133	8.77E-06	674	0.057
C1OC2	0.364	0.017	640	0.239
C2OC2	1.405	1.045	453	1.55
C2	0.487	9.00	369	62.1
C4	0.231	4.28E-03	616	0.440

The characterisation of the OER was also performed by the Arrhenius relation - eq 1 – shown in **Figure 12A**. The obtained OER E_a values are shown in **Figure 12B**. The addition of C1OC2 and C1OC2 significantly decreased the OER E_a, and the C2 IL reduced further the OER Ea. The C4 IL increased the OER E_a.

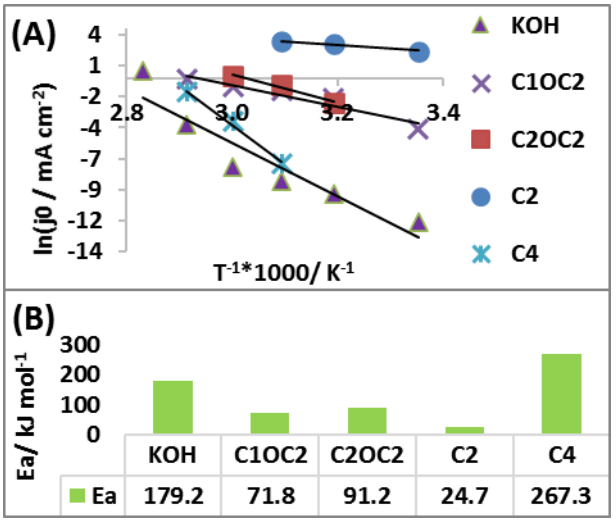

Figure 12. (A) OER Arrhenius plots for 8 M KOH solution without and with the addition of C1OC2, C2OC2, C2, and C4 ILs and (B) the corresponding OER activation energies.

3.3.4. OER Stability test

C2 IL result was not considered. Among the other ILs C4 performed the best having much higher current densities than C1OC1 and C2OC2. C4 curve shows an ascending trend, which is not in accordance with the expectations, and still shows lower current densities than KOH. KOH has a descending trend as expected, results shown in **Figure 13**. At 80ºC, none of the ILs

facilitated OER. Furthermore, the addition of ILs results in at least 3 times lower current densities. The KOH curve has an unexpected increasing trend in the beginning, and it slightly started to ascend just in the second half of the experiment.

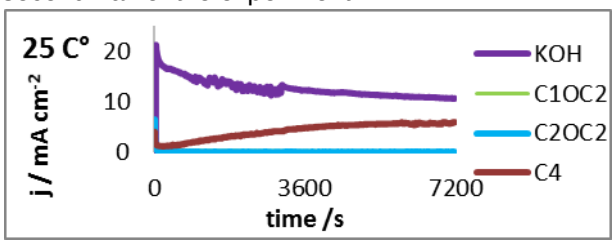

Figure 13. 2h-long stability test on 1.92 V at 25ºC in pure 8 M KOH solution and with the addition of C1OC2, C2OC2, and C4 ILs.

For better comparison, KOH data were taken away. Among ILs C2 performed the best, which was followed by C1OC2 IL. Each curve has an ascending trend, C2 has a square root shape, meanwhile C1OC2 has a square shape. These ILs highly overperformed C4 and C2OC2. C4 and C2OC2 have similar ascending trends and amplitude. Each IL curves have an ascending trend, which was unexpected. OER stability test results are shown in **Figure 14**.

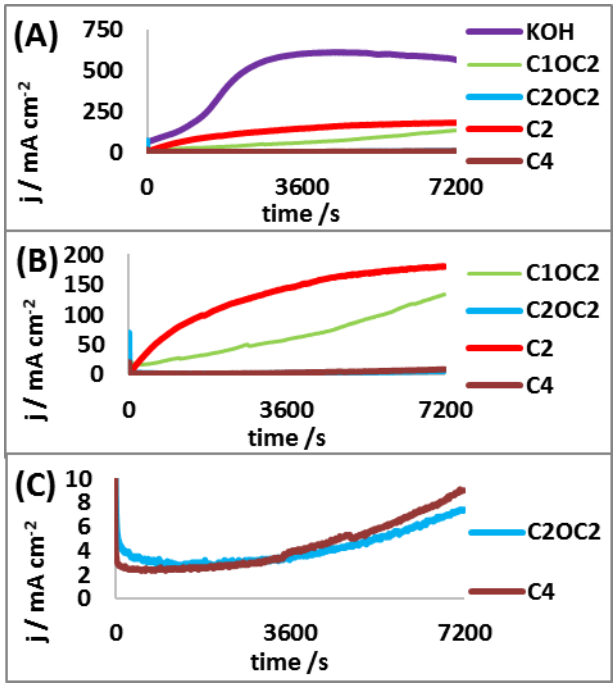

Figure 14. 2h-long stability test at 1.92 V at 80ºC in (A) pure 8 M KOH and in 8 M KOH upon addition of C1OC2, C2OC2, C2 and C4 ILs; (B) Excluding KOH data for better overlook of other results; (C) Excluding KOH, C2 and C1OC2 data for better overview of the other results.

3.4. Volume measurements

3.4.1. Summary of fundamental measurements

For the gas volume measurements, evaluating the performance of the ILs and chose the best one was needed. However, there were no ILs that unequivocally outperformed the others. Although during the OER experiments, the outstanding results of C2 are proposing the chance of measuring failure, in case of the lack of samples to repeat the C2 OER measurements, finally we chose C2 as the best performing IL because of the following: -C2 performed the best during LSV of HER; -C2 had the highest current densities at the beginning of the HER stability tests; -C2 looks more stable comparing to other ILs according to HER data; -During LSV of OER at 25 ºC C1OC2 and C2OC2 performed the worst; -During stability test of OER at 25 ºC C1OC2 and C2OC2 performed by far the worst as well.

3.4.2. Constant current measurements

During the chronopotentiometry test, at a constant current of 800 mA, which corresponds to 35.7 mA cm^{-2}, the pure KOH solution without the C2 IL addition performed better. The C2 IL addition fastened the increment of the potential; however, the starting potential was lower in the case of C2 addition see in **Figure 15**.

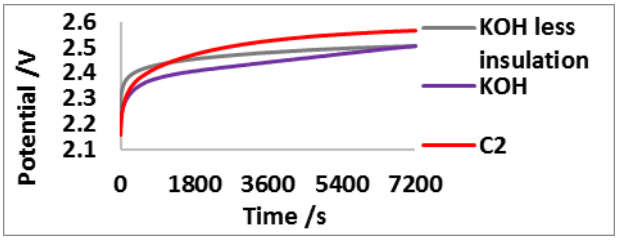

Figure 15. Comparison of pure 8 M KOH solution with and without the addition of C2 IL, during chronopotentiometry, where 800 mA were applied, corresponding to 35.7 mA cm^{-2}. KOH fewer insulation data refers to the use of one additional parafilm layer for sealing the electrolysis cell. KOH refers to the use of double parafilm layer for sealing) with y axis from 2.1 to 2.6 V.

During the first chronopotentiometry test, the theoretically calculated gas volume based on the applied current was more than the volume measuring device detected. Thus, indicated a failure in the reinforcement of the sealing, which means an additional parafilm layer was applied over the cell gasket. Afterwards, when there was a parafilm layer under and over the cell gasket, the detected gas volume was in balance with the theoretically calculated gas volume. The measurements with the C2 IL addition were done with the reinforced sealing. The difference between the addition of C2 IL, and the pure KOH solution in terms of the produced gas volume are minor. Results shown in **Table 6** and **Table 7**.

Table 6. Comparison of CP results with the specified indicators. E is the total energy used; Q is the total charge applied; V_{theo} is the theoretical produced gas volume; $\eta_{theo-ell}$ is the theoretical electric efficiency; η_{VM} is the efficiency of volume measuring; η_{H_2} is the measured electric efficiency.

	KOH	C2	KOH less insulation
E[J]	14005	14380	14186
Q[C]	5753.0	5753.2	5749.9
$V_{theo}[STP\ dm^3]$	1.002	1.002	1.004
$V_N\ measured[STP\ dm^3]$	0.813	0.784	0.506
$\eta_{theo-ell}$	0.609	0.593	0.602
η_{VM}	0.811	0.782	0.504
η_{H_2}	0.494	0.464	0.303

The observations of chronoamperometry can be summarised in the following points:

- Using two layers of parafilm tape – one under and another one over the gasket – significantly increasing the measured gas volume.
- With C2mim addition 2.7 % more energy was used, comparing to without C2mim.
- With C2mim addition 3,5 % less gas was measured, comparing to without C2mim.
- With CT2mim addition the H_2 production was 6.1 % less efficient, comparing to without C2mim.
- With C2mim addition the overall resistance was 2.7 % higher, comparing to without C2mim.

Table 7. Comparison of the chronopotentiometry results by average current, average potential, and average resistance.

	C2	KOH	KOH less insulation
AVG Current / mA	799.7	799.7	799.8
AVG Potential / mA	2.50	2.43	2.47
Resistance /Ω	3.13	3.04	3.08

3.4.3. Constant potential

During the chronoamperometry test, the C2 IL additions resulted in a significant increase of the current compared to pure 8 M KOH solution. The C2 IL addition was increasing the starting current. The current was not decreasing faster than in the case of the pure 8 M KOH solution, and the difference between currents was constant, see in **Figure 16**. The first test of pure 8 M KOH with the less insulation performed slightly better than with the reinforced insulation, but the final currents were similar.

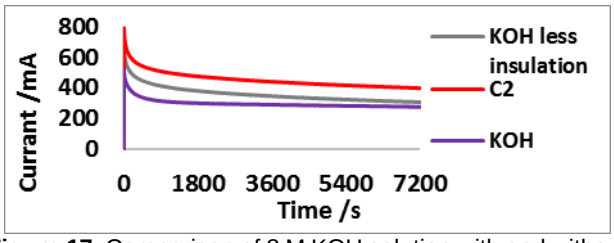

Figure 17. Comparison of 8 M KOH solution with and without the addition of C2 IL, during chronoamperometry at 2.3 V. KOH less insulation data refers to the use of one additional parafilm layer for sealing the electrolysis cell, meanwhile KOH refers to the use of a double parafilm layer for sealing.

The addition of C2 IL to the 8M KOH solution was significantly increased the volume flow rate as the volume flow rate follows a linear relationship with the current. In each case, the fast volume flow rate increment was followed by a short, but rapid decrease, and after that the volume flow rate was decreasing slowly. With the C2 IL addition, the volume flow rate was less stable, but still, it was significantly higher, which resulted in higher produced gas volume as well (**Figure 17**). The observations of chronopotentiometry:

- With C2mim addition 53.1 % more energy was used, comparing to without C2mim.
- With C2mim addition 37.4 % more gas was measured, comparing to without C2mim.
- With C2mim addition the H2 production was -10.2 % less efficient, comparing to without C2mim.
- With C2mim addition, the overall resistance was 34.7 % smaller, comparing to without C2mim.

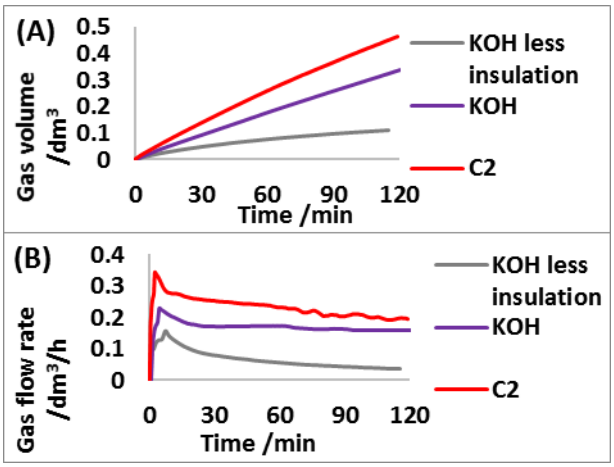

Figure 16. (A) Gas volume measuring results using 8 M KOH solution with and without the addition of C2 IL, during chronopotentiometry at 800mA, corresponding to 35.7 mA cm^{-2}. KOH less insulation data refers to the use of one parafilm layer for sealing the electrolysis cell, whereas KOH refers to using double parafilm layer for sealing. (B) Gas volume flow rate data using 8 M KOH solution with and without the addition of C2 IL, during chronopotentiometry.

It is important to note that with C2 IL addition, the current was significantly higher which could be explained by the C2 IL decreasing the resistance of the system. This evidences that C2 IL can significantly enhance water electrolysis. However, to compare the energy consumption, another device would be needed to measure how much energy was invested to maintain that constant potential. It is not clear why C2 performed better only during constant potential, whereas during the constant current the results are similar. Results are shown in **Table 8** and **Table 9**.

Table 8. Chronoamperometry results with the specified indicators. E as the total energy used; Q as the total charge was applied; $Vtheo$ as Theoretical produced gas volume; $\eta theo{-}ell$ as theoretical electric efficiency; ηVM as Efficiency of volume measuring; $\eta H2$ as Measured electric efficiency.

	KOH	C2	KOH less insulation
E[J]	4896	7494	5937
Q[C]	2128.8	3258.5	2581.3
$V_{theo}[STP\ dm^3]$	0.371	0.568	0.450
$V_N\ measured[STP\ dm^3]$	0.305	0.419	0.099
$\eta_{theo-ell}$	0.644	0.644	0.644
η_{VM}	0.822	0.738	0.221
η_{H_2}	0.530	0.476	0.142

Table 9. Chronoamperometry results by average current average potential and average resistance.

	C2	KOH	KOH less insulation
AVG Current / mA	435.7	284.5	358.6
AVG Potential / mA	2.27	2.27	2.30
Resistance /Ω	5.22	7.99	6.41

4. Conclusions

With the rising of temperature, each ILs started to decompose. This degradation had a negative effect on the reaction kinetics, during HER. The optimal temperature range is between 25 ºC and 40 ºC, above this range, the current density started to decrease, except in the case of C2. However, even with the negative effect of the decomposition, the addition of ILs enhanced HER kinetics by:

- Increasing peak current density, decreasing onset potential, and shifting OCP to more positive values during cyclic voltammetry
- Increasing the exchange current density, decreasing E_{10} potential, and increasing j_{150} current density during LSV tests at 25 ºC and 80ºC.

A strange phenomenon appeared when the current density was increasing during the stability test. This was also unexpected. It can be explained by measuring failure, but this increase at 80 ºC was measured four times again during the OER stability test at 80 ºC. It is also possible that the later intermediates have a catalytic effect too. Otherwise, if the later intermediates do not affect the HER kinetics, the current density should converge to the KOH curve. Therefore, further investigation of degradation is needed in form of longer stability tests at higher potentials. Also, the effect of intermediates of the ILs degradation is not clear as well. In summary of HER studies, ILs enhanced HER kinetics, in accordance with previous reports. Other ILs significantly worsen OER kinetics which resulted in smaller peak current densities during the CV test, and smaller current densities above 2.03 V on the LSV recorded at 25ºC. On the other hand - below 1.9 V - the OER reaction starts earlier with the addition of ILs. This can be explained by the assumption that IL ions would form a charge-separated layer formation, with a changing anion-cation rich layer at the electrode surface, whereas the proposition of the ions depends on the magnitude of the electrode surface. Therefore, on lower potential the concentration of the active cations close to the positively charged anode is higher, hence their catalytic effect is higher as well. On the other hand, the lower current densities with the addition of ILs above 2.03 V is not explained During LSV measurements for OER studies the OCP shifted to a more negative value, and the current density started to slowly increase much earlier – at 0.5V - comparing to pure KOH solution where the onset point was 1.5 V. The Tafel plots show an enhancing effect of ILs on OER kinetics by:

- Increasing the exchange current density, decreasing E_{01} potential, and increasing j_{500} current density during LSV tests on 25 ºC

ILs have a different performance at different potential levels, also each of them starts to degrade by the increasing temperature. The degradation has a negative effect on the reaction kinetics. However, during stability tests at 25 ºC and at 80 ºC current density increasing was observed. Therefore, further investigation on the degradation of ILs, and the effect of degradants on HER and OER is adequate. The proposed future properties of an IL ion that could catalyse the OER are the following:

- Having a bulky anion to get closer to the anode on higher potential values
- Having an amphipathic part which can help ions and the electrode surface to lose their solvation layer
- A molecule that can act as a hydroxide ion (OH^-) donor and acceptor; thus, the cation can take part in the electrochemical reaction and as a consequence, the cation is not blocking ECAS. Similarly, as the imidazolium$^+$ ion acts as a hydrogen ion (H^+) donor and acceptor.

According to volume measuring during chronopotentiometry, the addition of C2 resulted in 3.5% less gas production; 6.1% less hydrogen production efficiency, and 2.7% higher average resistance. On the other hand, during chronoamperometry, the addition of C2 resulted in: 37.4% more gas production; 10.2% less hydrogen production efficiency, and 34.7 % smaller average resistance. For further investigations, the volume measuring should be based on real-life industrial operation conditions, at around 200-400 mA cm^{-2} [9].

References

[1] M. David, C. Ocampo-Martínez and R. Sánchez-Peña, “Advances in alkaline water electrolyzers: A review,” *Journal of Energy Storage,* vol. 23, pp. 392-403, (2019).

[2] L. Amaral, D.S.P. Cardoso, B. Šljukić, D.M.F. Santos and C.A.C. Sequeira, “Room Temperature Ionic Liquids as Electrolyte Additives for the HER in Alkaline Media,” *Journal of The Electrochemical Society,* vol. 164, F427-F432, (2017).

[3] L. Amaral, J. Minkiewicz, B. Šljukić, D.M.F. Santos, C.A.C. Sequeira, M. Vranes and S. Gadzuric, “Toward Tailoring of Electrolyte Additives for Efficient Alkaline Water Electrolysis: Salicylate-Based Ionic Liquids,” *ACS Applied Energy Materials,* vol. 1 (9), pp 4731-4742, (2018).

[4] F. Fiegenbaum, M.O. Souza., M.R. Becker, E.M.A. Martini and R.F. Souza, “Electrocatalytic activities of cathode electrodes for water electrolysis using tetra-alkyl-ammonium-sulfonic acid ionic liquid as electrolyte,” *Journal of Power Sources,* vol. 280, pp. 12-17, (2015).

[5] G.-R. Zhang, T. Wolker, D.J. Sandbeck, M. Munoz, K.J.J. Mayrhofer, S. Cherevko and B.J. Etzold, “Tuning the Electrocatalytic Performance of Ionic Liquid Modified Pt Catalysts for Oxygen Reduction Reaction via Cationic Chain Engineering,” *ACS Catalysis,* vol. 8 (9), pp. 8244-8254, (2018).

[6] L. Zanchet, L.G. Trindade, D.W. Lima, W. Bariviera, F. Trombetta, M.O. Souza and E.M. A. Martini, “Cation influence of new

imidazolium-based ionic liquids on hydrogen production from water electrolysis," *Ionics,* vol. 25, pp. 1167–1176, (2019).

[7] R.F. Souza, G. Loget, J.C. Padilha, E.M.A. Martini and M.O. Souza, "Molybdenum electrodes for hydrogen production by water electrolysis using ionic liquid electrolytes," *Electrochemistry Communications,* vol. 10, pp. 1673-1675, (2008).

[8] J. Gao, L. Chen, Y. He, Z. Yan and X. Zheng, "Degradation of imidazolium-based ionic liquids in aqueous solution using plasma electrolysis," *Journal of Hazardous Materials,* vol. 263, pp. 261-270, (2014).

[9] Y. Guo, G. Li, J. Zhou and Y. Liu, "Comparison between hydrogen production by alkaline water," in *IOP Conference Series: Earth and Environmental Science 371*, Beijing, (2019).

[10] S. Nian-Tzu, H. Sung-Fu, Q. Quan, Z. Nan, X. Yi-Jun and M.C. Hao, "Electrocatalysis for the oxygen evolution reaction:recent development and future perspectives," *Chemical Society Reviews,* vol. 46, pp. 337-365, (2017).

[11] T. Muhammad, P. Lun, I. Faryal, Z. Xiangwen, W. Li, Z. Ji-Jun and L.W. Zhon, "Electrocatalytic oxygen evolution reaction for energy conversion and storage: A comprehensive review," *Nano Energy,* vol. 37, pp. 136-157, (2017).

[12] I.E.A."https://www.iea.org/weo2018/scenarios/, " 2019. [Online]. Available: iea.org/weo2018. [Accessed 25.9.2019].

[13] O. Takaya, T. Mizumoto and K. Yuya, "Analysis of Trends and Emerging Technologies in Water Electrolysis Research Based on a Computational Method: A Comparison with Fuel Cell Research," *sustainability,* vol. 10, pp. 478/1-478/24, 2018.

[14] S. Weidner, M. Faltenbacher, I. François, D. Thomas, J.B. Skúlason and C. Maggi, "Feasibility study of large scale hydrogen power-togas applications and cost of the systems evolving with scaling up in Germany, Belgium and Iceland," *International Journal of Hydrogen Energy,* vol. 43, pp. 15625-15638, (2018).

[15] E.U.N.F.C.O. Climate, "2019 United Nations Framework Convention on Climate Change," [Online]. Available: https://unfccc.int/sites/default/files/english_paris_agreement.pdf. [Accessed 30.09.2019].

[16] P. David and P.K. Martin, "Techno-economic implications of the electrolyser," I*nternational Journal of Hydrogen Energy,* vol. 41, pp. 3748-3761, (2016).

[17] I.E.A., "The Future of Hydrogen Report prepared by the IEA for the G20, Japan Seizing today's opportunities,"(2019).